ELSEVIER

International Journal of Coal Geology 46 (2001) 11–25

International Journal of COAL GEOLOGY

www.elsevier.nl/locate/ijcoalgeo

Quantitative coal characterisation by means of microfocus X-ray computer tomography, colour image analysis and back-scattered scanning electron microscopy

M. Van Geet [a,*], R. Swennen [a], P. David [b]

[a] *Afdeling Fysico-Chemische Geologie, Katholieke Universiteit Leuven, Celestijnenlaan 200C, B-3001 Heverlee, Leuven, Belgium*
[b] *NITG-TNO, Budapestlaan 4, P.O. Box 80015, NL-3508 TA Utrecht, Netherlands*

Received 24 May 2000; accepted 18 December 2000

Abstract

Microfocus computer tomography is a non-destructive technique enabling virtual slicing of opaque objects. Stacking several slices enables 3D visualisation of the object. To extract quantitative information, a thorough calibration with data obtained by classical microscopy techniques is needed. Correlation of microfocus computer tomography data with colour image analysis data of reflected-light microscopy and with back-scattered electron microscopy is worked out. SEM EDX is also used to identify mineralogical phases. Compared to former studies, much better resolutions were achieved in the order of 185 μm. Moreover, a dual energy technique is presented allowing the measurement of the density of all components. It is shown that macerals, which are abundant in the studied coal sample (i.e. vitrinite and liptinite in this study), can be quantified by microfocus computer tomography. However, no significant information on other components like pyrite and inertinite, which have surface percentages of less than 2%, could be retrieved from this sample. Finally, a close interrelation between liptinite and clay is demonstrated. With this information a 3D maceral and mineral visualisation and quantification is performed. In the studied sample 23% of the volume of the sample contains 90% of vitrinite together with 10% of another constituent. A 3D coal characterisation is thus possible.

Keywords: Tomography; X-ray analysis; Macerals; Coal; Colour image analysis; Electron microscopy

1. Introduction

Computer tomography, developed in medical sciences, is a non-destructive technique. The usefulness of the technique in geological research has been demonstrated by many authors (Wellington and Vinegar, 1987; Fabre et al., 1989; Raynaud et al., 1989; Swennen et al., 1990; Orsi et al., 1994; Boespflug et al., 1995; Verhelst et al., 1996; Duliu, 1999). Typical resolution of medical scanners is 500 μm within the slice and a slice thickness of 1 mm. This limitation of resolution restricts its application to identify small objects such as macerals in coal samples. Recent developments in X-ray tube production enabled the construction of microfocus computer tomography (μCT) instruments (Sasov, 1987;

* Corresponding author. Fax: +32-16-327-981.
E-mail address: Maarten.Vangeet@geo.kuleuven.ac.be (M. Van Geet).

0166-5162/01/$ - see front matter
PII: S0166-5162(01)00006-4

Fuhrmann, 1993), with significant enhancements in resolution. Simons et al. (1997) presented some enhanced results for coal characterisation by the use of this type of instrumentation. At that time, however, some instrumental limitations and artefacts still affected the final results. With respect to these former in-house studies, major advantages are achieved in this study. First of all, the resolution of the μCT data is significantly ameliorated. Second, the major artefact, namely beam hardening, considered the most important cause of error in the former studies, is minimised. Next, the resampling procedure is tuned to the μCT-resolution in order to achieve results at a far better resolution. Finally, a dual energy approach is implemented in order to extract data on physical density, which makes it easier to interpret data and provides a supplementary control of the acquired results.

This study focuses on the correlation of μCT data with colour image analysis data by means of multiple linear regression. The basic assumption in this study is that μCT data mainly depend on density of voxels and that the volumetric contribution of constituents influencing the voxel density as determined by microscopic techniques can be used to calculate the in situ density of different components. Such a correlation helps in correctly interpreting the acquired μCT data. The 2D surface data of classical optical microscopy and back-scattered electron microscopy are compared with a 2D μCT slice through a coal sample. This 2D correlation forms the basis for an extension towards 3D μCT data interpretation. As coal maceral and mineral composition is important for a large number of applications, for example, coal quality assessment for technical applications (Thomas, 1992), for environmental impact (Finkelman and Gross, 1999) and for coal bed methane extraction (Lamberson and Bustin, 1993; Laxminarayana and Crosdale, 1999), the technique of μCT is a promising tool for fast 3D quality testing of coal samples.

This paper gives a short description of the new developed microfocus computer tomography instrumentation and set-up. Special attention will be paid to the limitation of artefacts and the interpretation of the acquired data. Details on the equipment used and an outline of the concept are discussed. Subsequently, a correlation between those techniques is given for one coal sample. Finally, an extension towards 3D characterisation is given.

2. Microfocus computer tomography

The technique of microfocus computer tomography (μCT) enables the visualisation and quantification of the attenuation of X-rays within an object in three dimensions. This is done by illuminating an object from different angles with X-rays. The intensity of X-rays after passing through the object can be expressed by Beer's law:

$$I = I_0 \exp(-\mu h) \tag{1}$$

where I_0 is the intensity of X-rays emitted by the X-ray source, μ is the linear attenuation coefficient, and h is the thickness of the object. Consequently, differences in linear attenuation coefficient can be visualised. This linear attenuation coefficient depends on atomic number of the object (Z), density of the object (ρ), and the energy of the X-rays used (E), and can be expressed as:

$$\mu = \rho\left(a + b\frac{Z^{3.8}}{E^{3.2}}\right) \tag{2}$$

The first and second term of Eq. (2) correspond to the physical processes called Compton scatter and photoelectric absorption, respectively (Curry et al., 1990). A third process that occurs is Rayleigh scattering; however, this is, according to the latter authors, negligible and, consequently, is not incorporated in the equation.

By taking X-ray radiographs of the object from many different angles, a 3D reconstruction of the object can be achieved. Several algorithms can be used to reconstruct virtual slices through the object, which enables a visualisation of the distribution of several features of different linear attenuation coefficient. One of the most widely used reconstruction techniques is filtered back projection (Brooks and Di Chiro, 1976; Herman, 1980; Kak and Slaney, 1988).

Compared to conventional CT, microfocus computer tomography allows for an improvement of resolution. This is achieved by reducing the size of the X-ray source, which leads to the reduction of the unsharpness (blurring) at the detector. Consequently,

the object can be placed near the X-ray source, with no significant lack of sharpness. This leads to the detection of a primary enlargement of the object and enhanced resolution. The best resolution that can be achieved is about the size of the focal spot of the X-ray source, currently about 10 μm. Since a point source of X-rays and a 2D detector are used, this resolution can be achieved in all three dimensions.

In the final image, every pixel represents the mean linear attenuation coefficient of that volume of the sample. Consequently, features smaller than the limit of resolution are not resolved, but their contribution of density and atomic number is incorporated in the final image. The final visualisation of the μCT data is a 2D image. Every pixel, actually, represents information of a 3D voxel. In what follows, the term pixel and voxel will be used mutually for μCT data, but it should be kept in mind that it physically always represents a voxel.

The technique of microfocus computer tomography has one severe artefact, namely beam hardening (Joseph, 1981). As stated in Eq. (2) the linear attenuation coefficient depends on the X-ray energy. However, as polychromatic X-ray sources are used in commercial (μ)CT-instruments, the energy changes while travelling through the object, whereby the low X-ray energies are preferentially absorbed. The more absorbing the material, the more pronounced this artefact will be. This spectral shift of the X-ray energy results in the creation of high-attenuating object rims, while the central part is less attenuating (Van Geet et al., 2000). Several techniques for minimisation or elimination of the beam-hardening artefact have been described in literature (Stonestrom et al., 1981). However, for most of them, an a priori knowledge of the composition of the object is necessary. As this is quite difficult for coal characterisation, the use of hardware metal filters cutting off the low X-ray energies is recommended for geological research (Jennings, 1988; Van Geet et al., 2000). This technique diminishes the beam hardening artefact in high attenuating materials and nearly excludes the beam hardening artefact in less attenuating materials, like coal (Van Geet et al., 2000).

Finally, the linear attenuation coefficient is difficult to interpret in geological materials. Therefore, a technique of dual-energy has been worked out, in order to extract information about physical density of the rock constituents. From Eq. (2) it can be deduced that for two different energies:

$$\mu_h = \rho\left(a_h + b_h \frac{Z^{3.8}}{E^{3.2}}\right)$$

$$\mu_l = \rho\left(a_l + b_l \frac{Z^{3.8}}{E^{3.2}}\right) \quad (3)$$

where subscript h and l refer to the high and low energy scans, respectively.

A calibration with materials of known density and atomic number enables to extract the parameters a_h, a_l, b_h and b_l. Once this calibration is completed, the equations can be rewritten to extract density and atomic number from any component (Coenen and Maas, 1994; Van Geet et al., 2000). This procedure is, however, sensitive to noise.

3. Methodology

In this study we investigate a subsample of the sample used in Verhelst et al. (1996) and Simons et al. (1997). This sample, from seam 20 (KS54) at a depth of 1108.54–1108.68 m from the Peer borehole (KB 206) in the Campine Basin (NE Belgium) was chosen as to be able to compare with the results of those two previous studies. The seam is identified as Westphalian A (Wenselaers et al., 1996) and classified as high volatile A bituminous coal with a vitrinite reflectance of 0.97% R_r. The well was drilled for a pilot project for research on the possibilities of coal bed methane extraction in the Campine Basin.

From the original impregnated sample with one polished surface, a subsample of 8 mm in diameter was drilled. On the polished surface two traces, perpendicular to the compositional banding, were analysed by colour image analysis (CIA) over a length of approximately 7 mm. Each trace was composed of about 38 images of 768 × 576 pixels, each pixel about 0.35 × 0.35 μm in size. The instrument used in this study was a SIS PRO Colour Image Analysis System equipped with a Sony DXC-930 RGB video camera, a Acerview76e monitor (1024 × 1024 pixels), and a Zeiss Axioplan microscope with an Epi-Plan 50 × oil immersion objective. This signal of the scanned image is transmitted to the hard-

ware of the SIS PRO using a PC-Pentium II computer and can then be used for different image operations.

In this study, the technique of CIA uses RGB intensity values or HIS (hue, saturation, intensity) information to distinguish between objects of different colour. The different constituents of coal can be differentiated by means of thresholding (David and Fermont, 1993), i.e. defining the upper and lower levels of the colour parameters of each group. This technique enabled the distinction between the three main groups of macerals, namely: vitrinite, liptinite, and inertinite. Moreover, pyrite and binder can be distinguished as well. The colour characteristics of pyrite and inertinite are sometimes very similar, potentially inducing an error. The instrument is not equipped with a motorised stage. Therefore, the transport of the sample has been performed manually, which undoubtedly introduces some errors.

Just beneath the polished surface a μCT slice was made. The instrument used is the Skyscan 1072 X-ray microfocus computer tomograph of the Katholieke Universiteit Leuven. The sample was scanned at 130 and 100 kV, both at 300 μA. Projections were taken over 180° with increments of 0.9°. Total scanning time is about 3 h. For both energies, a beam-hardening filter of 0.8 mm of aluminium and 0.1 mm of a CuZn alloy was used in order to reduce or eliminate artefacts.

Therefore, it can be assumed that X-ray energy is not changing while travelling through the coal sample. The basic assumption in this study is, however, that the linear attenuation coefficient linearly depends on density only for a given X-ray energy. This is only valid if the mean atomic number of the three coal components is similar, which is the case. Consequently, a correlation between linear attenuation coefficient and colour image analysis can be worked out. Compared to Simons et al. (1997), this study has a better resolution and the beam hardening is eliminated. The latter authors considered this artefact the most important cause of error. The dual-energy technique used furthermore enables to extract physical densities of all distinguishable constituents, which is much easier to interpret than linear attenuation.

The reconstruction used was a filtered back projection, which resulted in images of 512×512 pixels, each pixel about 21.7×21.7 μm in size. This results in a resolution enhancement of nearly a factor 2.5 compared to the study of Simons et al. (1997), where pixel size was 53×53 μm.

In order to investigate the mineral matter present in the coal sample, the polished section was coated with carbon and one trace was studied with backscattered electron (BSE) microscopy. The instrument used is a JEOL-JSM 6400 scanning electron microscope. Operating conditions were 15 kV, 60 μA, and about 600 Å beam width. The resulting images were digitally stored as 618×618 pixels, each pixel about 0.12×0.12 μm in size. Again, a non-motorised stage was used, which might introduce errors. This technique of BSE enables distinction of components of different atomic number, but additional chemical analysis allowed mineralogical identification. The latter was carried out by using an exL-LINK energy dispersive X-ray analytical system (EDX) on the scanning electron microscope. The difference in mean atomic number of the several coal macerals is, however, too small to allow differentiation between them. The only components that can be visualised here, are clay minerals and pyrite.

4. Data processing

The necessary conditions and operations needed for correlating data gathered from two different techniques is explained in detail in Simons et al. (1997). A similar approach is used here and is illustrated in Fig. 1.

Since the sampling intervals of the three techniques are different, a resampling procedure has to be applied. Simons et al. (1997) applied a resampling method, where the new μCT pixels cover the same surface area as one image in the CIA (100×100 μm^2). This leads, however, to serious loss of resolution for both techniques, CIA and μCT. In this study, the resampling is performed on the CIA and BSE images. They are resampled in blocks of 62×62 and 185×185 pixels, for CIA and BSE, respectively. All data now cover about 21.7×21.7 μm^2 with a maximum deviation between the three techniques of 1.85%. A resolution enhancement of factor 20 results with regard to the study of Simons et al. (1997). After resampling, the frequency content of both techniques should be approximately the same.

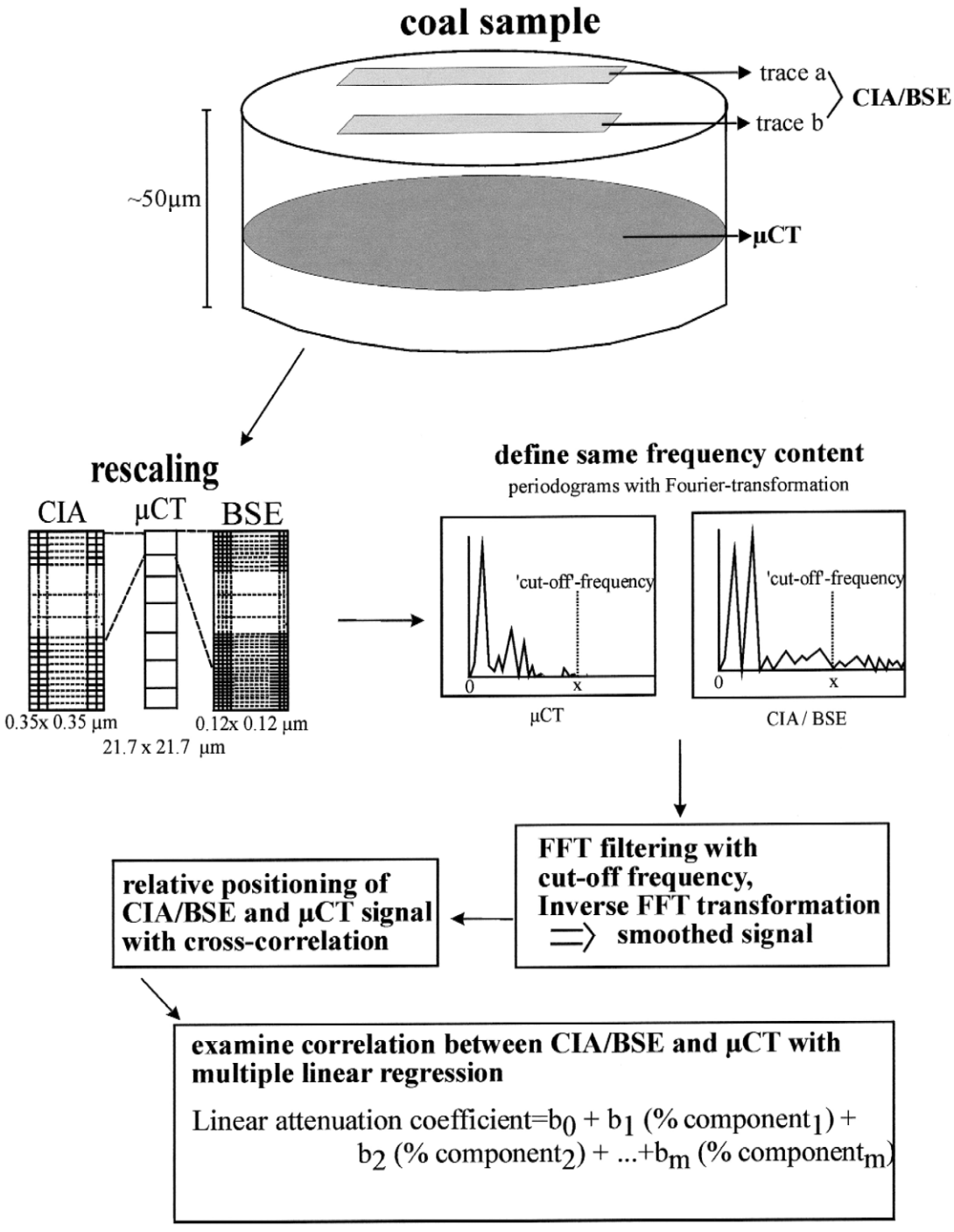

Fig. 1. Schematic overview of the different steps necessary to correlate the Colour Image Analysis (CIA) and Back Scattered Electron (BSE) data with the Microfocus computer tomography (µCT) data.

Table 1
Composition of the investigated coal as determined on two traces perpendicular to the maceral banding by means of colour image analysis (CIA)

Component	Normalised mean surface percentage (%)
Vitrinite	54.9
Liptinite	35.9
Inertinite	1.4
Pyrite	0.2
Binder	7.6

Therefore, the periodogram of each data set is calculated. The maximum frequency of the data set with the lowest frequency content is defined as the cut-off frequency. The frequency content of all data is limited to the same frequency content by FFT-filtering the data with the defined cut-off frequency. An inverse Fourier Transform allows reconstructing a smoothed version of the original data. Once these smoothed data are available, the mutual position of the data should be defined. Therefore, a local maximum of the cross-correlation between the data is sought.

As stated before, the basic assumption of this study is the linear correlation of the linear attenuation coefficient and the physical density. The latter depends on the composition of the coal, which in this study is expressed as the surface percentage of the constituents. Consequently, the following equation can be set up:

$$y = b_0 + b_1 x_1 + b_2 x_2 + b_3 x_3 + \ldots + b_m x_m + e. \quad (4)$$

where y is the linear attenuation coefficient, x_1 to x_m are the surface percentages of constituents identified by colour image analysis or back-scattered electron microscopy and b_0 to b_m are parameters. The coefficient e is an error term, which should be minimised by ordinary least squares in order to achieve the parameters b_0 to b_m. The coefficient of multiple determination R^2 is a measure of the percentage of the variability of the data that is explained by the regression model vs. the total amount of variability of the data. To work out this multiple linear regression by means of ordinary least squares, some conditions and assumptions should be met (Harnett and Murphy, 1980). First, all variables should be normally distributed and the independent variables x_1 to x_m must be mutually independent. The latter might cause problems in this study, as it is most likely that the surface percentage of vitrinite is negatively correlated with the surface percentage of liptinite. This is checked by calculating the correlation matrix. If there is no mutual independence, only one of both can be used as an independent variable. In that case, some information about the other constituent is still retrievable from the constant parameter b_0 in Eq. (4). Next, the error term should be independent of each of the independent variables, the errors should be normally distributed, the expected value of the errors should be zero and there variance should be constant. Finally, any two errors should be independent. The latter means there should be no autocorrelation or no systematic pattern in the error term. This could also be a problem in this study because of the banded structure of the coal.

5. Results

The mean composition of the investigated coal sample, as determined with CIA, is given in Table 1.

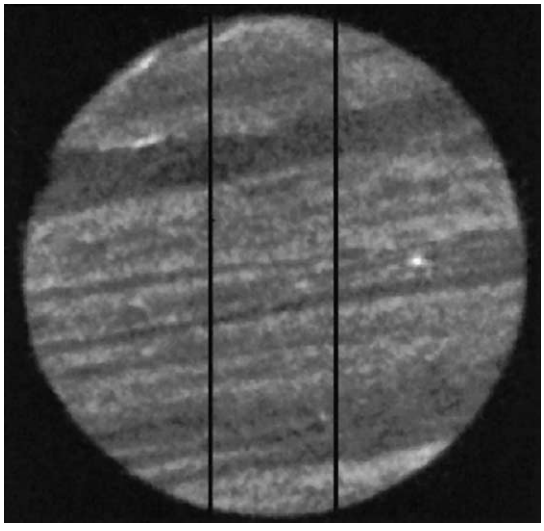

Fig. 2. μCT reconstruction through coal sample of 8 mm in diameter at 130 kV. A dark colour corresponds with low X-ray attenuation, while a whitish colour indicates material with high attenuating characteristics. The vertical black lines correspond with the position of the traces analysed with colour image analysis and back-scattered electron microscopy.

Table 2
Comparison of spatial resolution and sample diameter of several studies devoted to coal characterisation by means of (μ)CT

	Verhelst et al. (1996)	Simons et al. (1997)	This study
Spatial resolution (μm)	1400	667	185
Sample diameter (cm)	2.5	1.5	0.8

First, the results of the correlation between 2D μCT data and 2D colour image analysis and back-scattered electron microscopy is presented. A statistical discussion of this correlation follows. These data are consequently used for the extension towards 3D coal characterisation by means of μCT.

5.1. 2D μCT data

Fig. 2 shows the used μCT slice through the coal sample, scanned at 130 kV together with the position of the traces analysed with CIA and BSE. The compositional banding can be clearly distinguished. The periodogram shows that no significant frequency components above 185 μm occur. The CIA and BSE data, however, possess higher frequencies. Consequently, the cut-off frequency is set at 185 μm. As this cut-off frequency is related to spatial resolution, it can be used to compare it with former studies (Table 2). The achieved enhanced spatial resolution is, however, at the expense of sample size.

5.2. Cross-correlation μCT-CIA

In the CIA analysis, not all pixels can be classified as one of the sample constituents. For optimal data treatment, the whole signal is normalised. To be able to perform a multiple linear regression, the data are also smoothed by FFT-filtering the frequency content with a cut-off frequency of 185 μm (Fig. 3).

To position the μCT with respect to the CIA data, a maximum in the cross-correlation between the surface percentage of the linear attenuation coefficient and vitrinite is sought. Vitrinite was chosen since it is the most abundant coal component. Therefore, the largest variation in linear attenuation is probably related to this component.

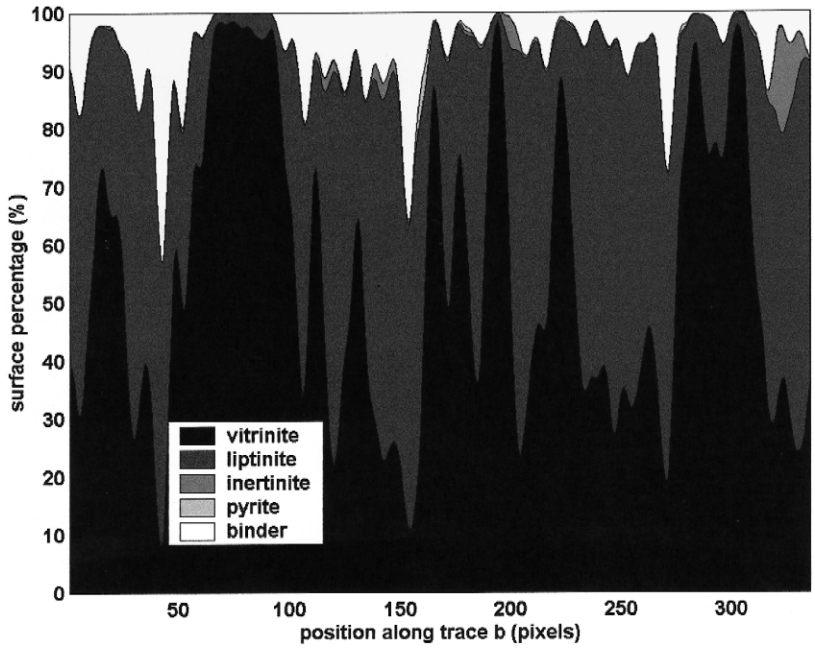

Fig. 3. Smoothed and normalised accumulated surface percentages of all constituents, discerned by CIA, for trace b. Because of the very low amounts of pyrite (less than 1%), it is very difficult to differentiate this component in this figure.

Subsequently, a multiple linear regression is performed with these data. As an illustration, the smoothed μCT signal is given together with the predicted values based on the CIA data for trace b in Fig. 4. Traces a and b consist of 331 and 336 data points (samples), respectively. The formulas for both traces (at 130 kV) are given below.

trace a: linear attenuation coefficient

$$= (0.0266 \pm 0.0006) + (0.0223 \pm 0.0014) \times (\mathrm{LIP}) + (0.0148 \pm 0.0044) \times (\mathrm{INE}) + (0.1061 \pm 0.0568) \times (\mathrm{PYR}) + (0.0137 \pm 0.0020) \times (\mathrm{BIN}) \quad (5)$$

trace b: linear attenuation coefficient

$$= (0.0293 \pm 0.0005) + (0.0195 \pm 0.0031) \times (\mathrm{LIP}) + (0.0508 \pm 0.0103) \times (\mathrm{INE}) + (0.0509 \pm 0.0469) \times (\mathrm{PYR}) - (0.0036 \pm 0.0035) \times (\mathrm{BIN}) \quad (6)$$

where LIP, INE, PYR and BIN denote the surface percentages divided by 100 of liptinite, inertinite, pyrite, and binder, respectively. The uncertainties quoted are standard errors of the regression coefficients. The coefficient of multiple determination (R^2) between the μCT signal and the predicted signal on all samples is 0.53 and 0.52 for traces a and b, respectively.

5.3. Statistical evaluation

As mentioned before, a multiple linear regression can only be applied as some conditions are met. Statistical techniques will be used to check these conditions and adapt the multiple linear regression technique in case one of the conditions is not true. In this paragraph, we concentrate on trace b, but similar results are obtained for trace a.

The amount of pyrite and inertinite is very low and very localised as can be deduced from Fig. 3. The question thus rises whether these components have a significant effect on the multiple linear regression analysis. Consequently, the coefficient of multiple determination and Mallow's c test are used to discriminate a good subset of variables (Weisberg,

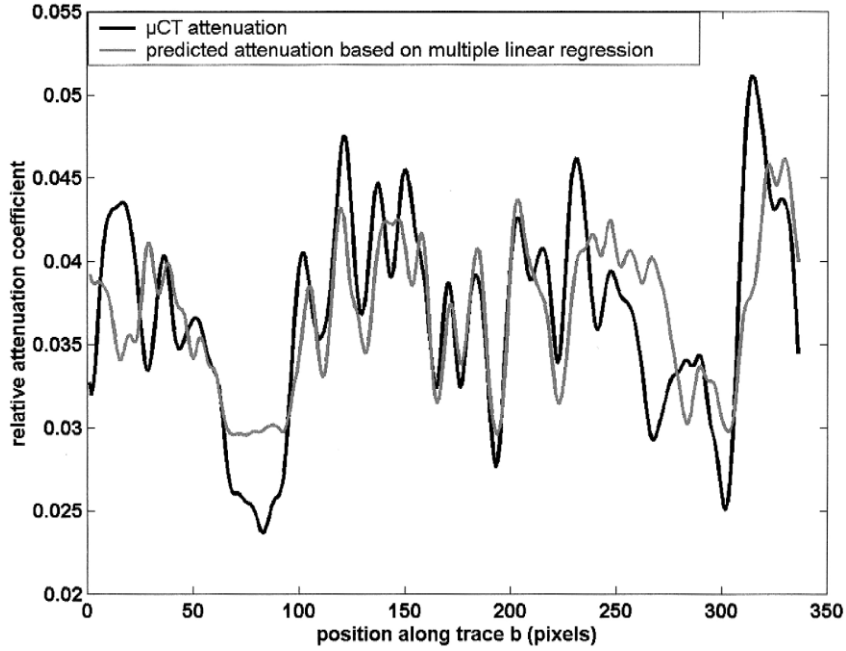

Fig. 4. Original μCT signal along trace b, together with the predicted attenuation values, based on the multiple linear regression with CIA data.

1980). This analysis shows that liptinite and binder are the most important parameters and explain most of the variances. The following equation is obtained for

$$\text{trace b: linear attenuation coefficient} = (0.0294 \pm 0.0005) + (0.0252 \pm 0.0016) \times (\text{LIP}) - (0.0090 \pm 0.0041) \times (\text{BIN}) \quad (7)$$

The obtained regression coefficients only slightly change with the values obtained before and the coefficient of multiple correlation (R^2) is 0.49 for trace b. From this it can be concluded that the sample used in this study is not suited for deducing any information on attenuation coefficient or density of pyrite and inertinite, as their contribution to the final result is statistically of minor significance. The following discussion is consequently restricted to the multiple linear regression of μCT data with liptinite and binder data of the CIA analysis. Information on vitrinite can still be found in the constant term.

A first condition is that all variables are normally distributed. This condition is better met if the μCT data are divided in two subpopulations and two different regression equations are defined for the two subpopulations. This is known as piecewise linear regression and leads towards an enhanced correlation, i.e. R^2 value of 0.79 for trace b. This corresponds with a correlation coefficient (R) of 0.89 (Fig. 5).

Another condition is that all systematic information is incorporated in the regression model. Autocorrelation is a systematic pattern in the errors and is most likely here because of the banded nature of the coal sample. The Durbin–Watson test can be used to check for such an autocorrelation (Harnett and Murphy, 1980) and in this case positively indicates such a serial autocorrelation. When the autocorrelation is not too severe, a generalised least square technique can be applied, but in this case the autocorrelation is too strong. Simons et al. (1997) already suggested a geostatitistical approach to find the extent of the serial autocorrelation. For more information on geostatistics and semivariograms, we refer to Journel and Huijbregts (1978) and Middleton (2000). Once the serial extent of autocorrelation is known, the data points can be resampled at a larger interval. The semivariogram of trace b (Fig. 6) was interpreted as

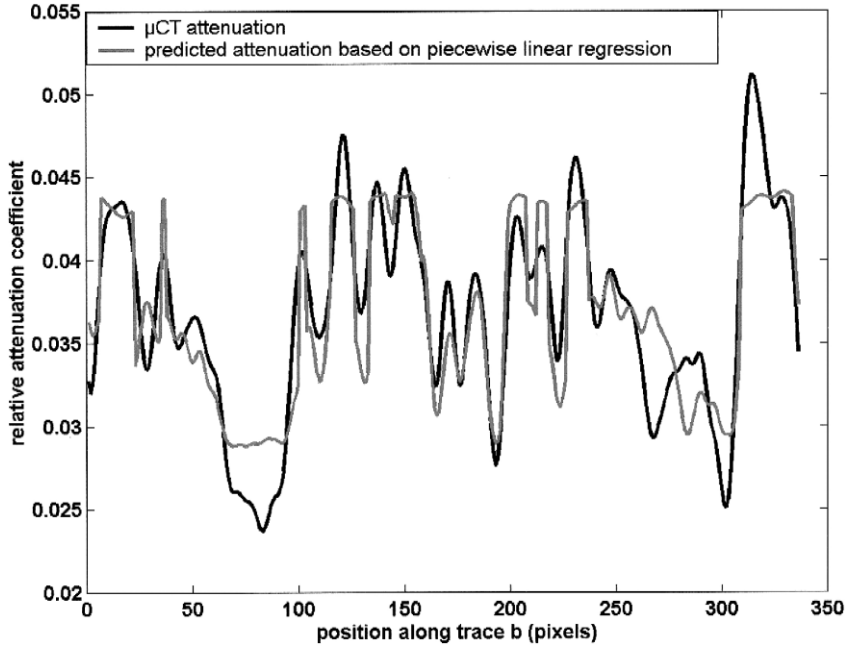

Fig. 5. Original μCT data, together with the predicted linear attenuation coefficients determined by means of piecewise multiple linear regression on CIA data for trace b.

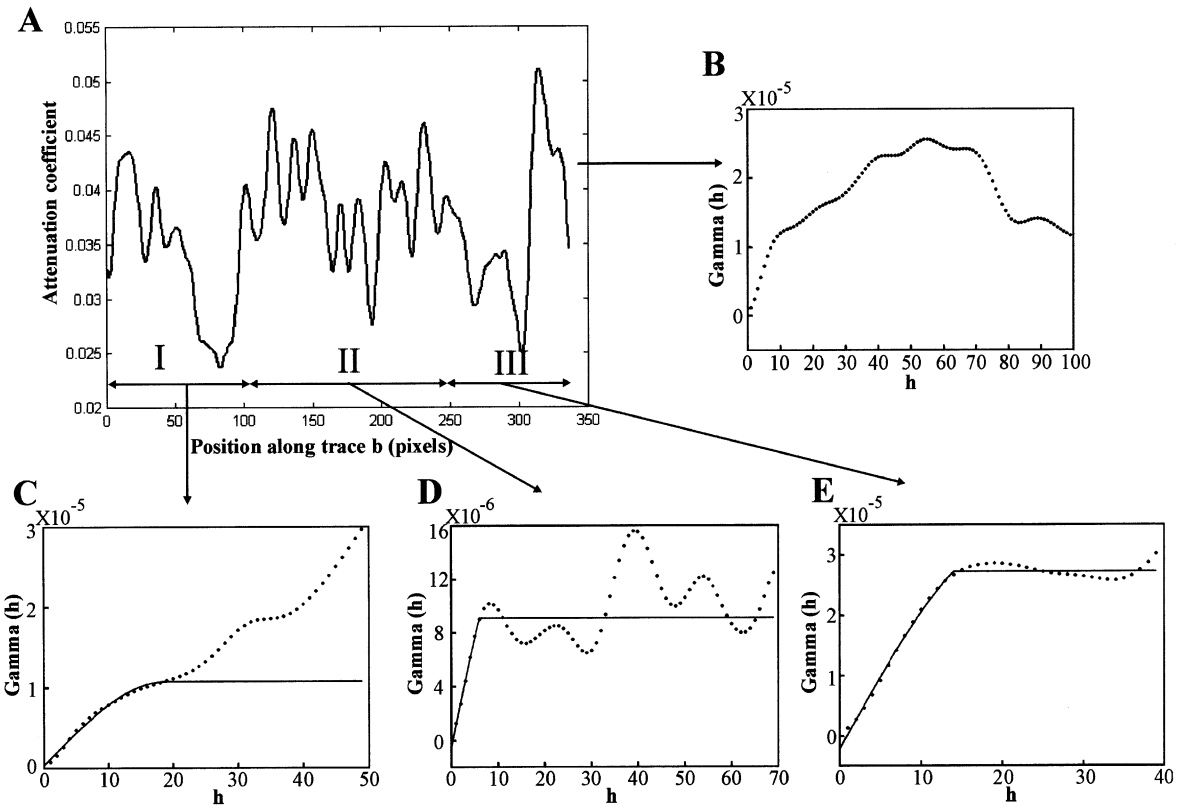

Fig. 6. Linear attenuation coefficient profile along trace b (A) together with the semivariogram for this profile (B) and semivariograms, overlain with a theoretical spherical model, of the three subparts indicated as I (C), II (D) and III (E).

a gigogne structure, which means two structures are superpositioned. This seems reasonable, as a visual inspection of trace b (Fig. 6) shows large bandings at the border and very small bands in the center. Therefore, the trace was split in three parts, indicated in Fig. 6. The semivariograms of those parts are also given in Fig. 6. These experimental semivariograms can be fitted with a theoretical spherical model, which gives an idea about the extent of serial autocorrelation, i.e. 20, 6, and 14 data points for the first, second, and last part, respectively. Subsequently, a resampling is performed, which results in 21 traces of 4 or 5 data points for the first part, 7 traces of 21 or 22 samples for the second part and 15 traces of 5 or 6 samples for the last part. On these different traces a multiple linear regression is performed, which leads to correlation coefficients R between 0.59 and 0.99 and coefficients of multiple determination between 0.35 and 0.98. A weighted average of all these correlations is calculated, using the reciprocal of the standard error as weights, which results in the following formula:

$$\text{linear attenuation coefficient} = (0.0269 \pm 0.0015) + (0.0381 \pm 0.0061) \times (\text{LIP}) - (0.0518 \pm 0.0154) \times (\text{BIN}) \quad (8)$$

It follows that adapted statistical techniques lead to better correlations and coefficients of determination.

5.4. Density calculation of constituents

In this study, the dual-energy technique enables to quantify physical density. This technique is quite sensitive to noise and to minimise the latter, the mean value of 10 succeeding slices (about 215 μm total thickness) was calculated. This procedure seems

justified since from a 3D reconstruction of the whole sample (Fig. 7) it was concluded that the compositional banding was continuous in the third dimension. Thus, smoother signals were achieved, enabling density measurements by means of the dual energy technique. The results, together with values given in literature, are shown in Table 3.

For vitrinite and binder, the calculated values are very close to the values given in literature. The calculated density of pyrite deviates somewhat from the values given in literature. The value for inertinite is quite different. As mentioned before, these constituents occur only very locally and are statistically not really relevant for the multiple linear regression analysis. Consequently, it can be accepted that their calculated densities are statistically not reliable. Moreover, the CIA-differentiation between pyrite and inertinite is not obvious. Finally, some of the inertinite lumms can be mineral filled, although it could not be checked. These facts might to a certain extent explain the overestimated calculated density of inertinite.

The calculated density of liptinite is also overestimated. This deviation was also found in the study of Verhelst et al. (1996) and Simons et al. (1997). Liptinite, however, is a major component, which easily can be differentiated with CIA. However, liptinite can occur in close interrelation with clay mineral matter. This is verified by means of backscatter electron (BSE) microscopy.

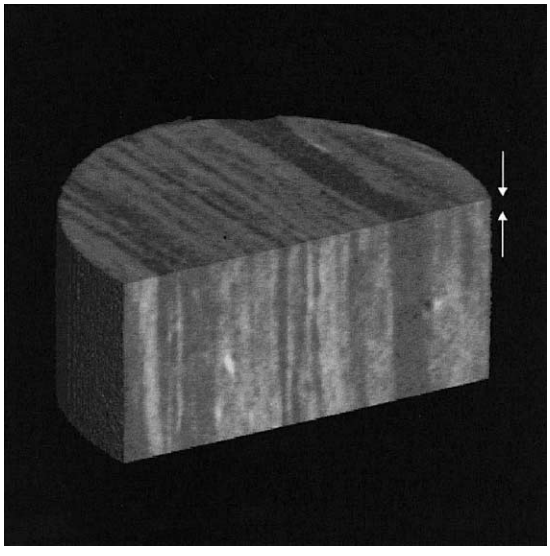

Fig. 7. Three dimensional visualisation of the studied sample. The third dimension is visualised along trace b. It can be concluded that an averaging procedure of the first 10 slices (between the two arrows) along the third dimension is justified, since the compositional banding does not change much in this direction.

Table 3
Comparison of the density measurements by means of dual-energy μCT and literature data for major coal constituents

Component	Calculated density (g/cm^3)	Literature (g/cm^3) (Stach et al., 1975)
Vitrinite	1.31	1.3
Liptinite	1.74	<1.3
Inertinite	5.64	1.6
Pyrite	4.66	5
Binder	1.21	1.2

5.5. Cross-correlation μCT–BSE

BSE is an outstanding technique in characterising mineral matter in coal. Moreover, the EDX equipment allowed quantifying the amount and the distribution of clay minerals. The frequency content of the resulting BSE signal is FFT-filtered with the above mentioned cut-off frequency of 185 μm. To position the BSE signal, the cross-correlation between surface percentage of clay and linear attenuation coefficient was maximised. This approach is justified by the fact that even a small amount of clay (with higher density and higher atomic number than coal components) will cause an increase in the linear attenuation coefficient.

The clay signal together with the liptinite signal, derived with CIA, is given in Fig. 8. It can be seen that high amounts of clay often correlate to the occurrence of liptinite. Unfortunately, it is not possible to incorporate the BSE-signal into the CIA-signal, since the clay matter accounted for one of the constituents in the latter technique. Consequently, only a semi-quantitative approach can be used. From this data set the mean surface percentage of clay within pixels with high liptinite content (pixels with more than the mean liptinite content) is about 20% to 30%. If a mean density of clay of 2.6 g/cm^3 is

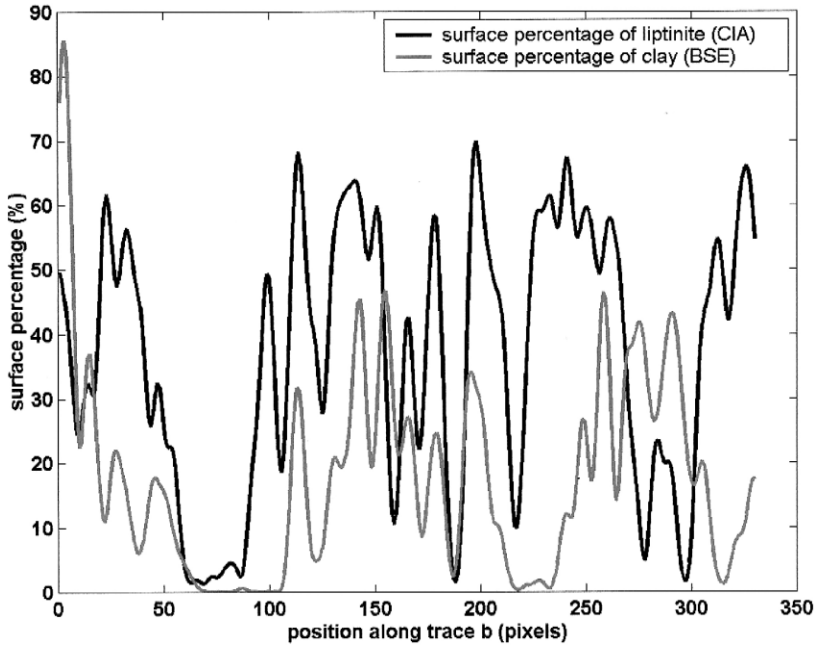

Fig. 8. Smoothed and normalised surface percentage of liptinite along trace b determined by CIA, together with the smoothed surface percentage of clay along trace b determined by BSE. Unfortunately, it is not possible to incorporate the BSE-signal into the CIA-signal, since the clay matter accounted for one of the constituents in the latter technique.

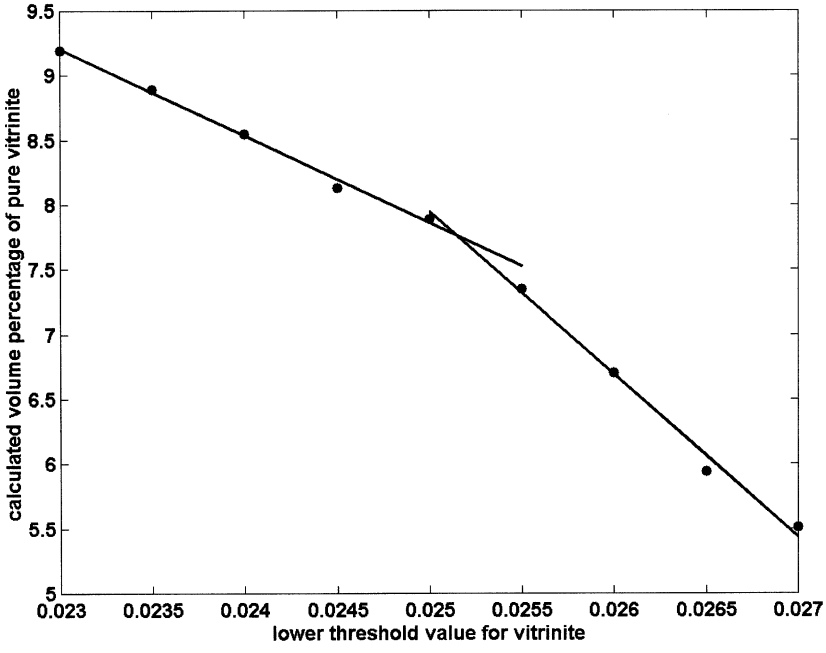

Fig. 9. The change of calculated volume percentage of vitrinite caused by changing the lower threshold value. The upper threshold value is kept constant at 0.0294. Two subpopulations with a linear trend can be discriminated. The intersection of the two linear trends can be assumed a good estimator of the lower threshold value.

assumed, the resulting density of liptinite given in Table 3 lowers to values reported in literature.

5.6. 3D coal characterisation

The cross-correlation performed now provides the basic data to visualise and quantify coal macerals within three dimensions in the sample. The regression constants can be used as threshold values for coal components, for example, vitrinite. Several regression equations are given and it is deduced that the regression constants vary slightly. The upper threshold value is kept constant at 0.0294. However, the effect of changing the lower threshold value in estimating the amount of vitrinite is checked and illustrated in Fig. 9. This effect can be divided in two linear trends. The first trend (threshold value 0.0230 to 0.0255) has a much smaller slope than the second trend (threshold value 0.0255 to 0.0270). The gentle slope might be caused by some small increase in volume percentage due to some random voxels, which might be interpreted as noise. Consequently, the intersection of the two linear trends (0.0250) might be a good choice of threshold value. Within the studied sample a volume of about 7% of voxels containing 100% vitrinite could be calculated. Voxels containing 90% vitrinite together with 10% of another constituent, make up about 23% of the sample volume. A change in the lower threshold value results in a difference of only 1%. The distribution of these voxels is visualised in Fig. 10, using a lower threshold value of 0.0260. The vitrinite banding can be clearly distinguished in three dimensions.

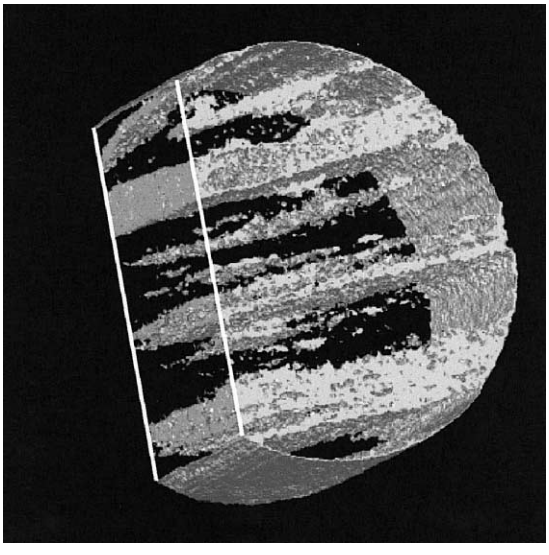

Fig. 10. Three-dimensional visualisation of the voxels containing 90% of vitrinite and 10% of another constituent. The outer border of the cylindrical object is also visualised.

6. Perspectives

This study illustrates the possibilities of μCT for coal quantification. The acquired data are very useful for sedimentological characterisation of coal seams, as vertical and lateral variations of coal constituents can be easily detected in 3D. Moreover, the amount of different constituents can be calculated and used, for example, in exploration studies of coal bed methane projects and in general coal quality assessments. Such projects also need quantitative data about fracture and cleat volumes and orientation. Research in progress focuses on the possibilities of fracture size determination within coal samples. Moreover, a quick overall view of mineral constituents can be established, which is an important parameter for coal bed methane projects and for coal quality studies. The determination of pyritic sulphur is probably an easily assessable and interesting parameter.

Finally, former studies that used lower resolution instruments revealed similar results, but attributed the discrepancy of the calculated liptinite value to the beam hardening artefact. From this study, it is clear that beam hardening is not causing this anomaly, but it is related to the impossibility of measuring the surface percentage of clay by means of colour image analysis. Consequently, the three levels of resolution (Verhelst et al., 1996; Simons et al., 1997; and this study) are complementary and demonstrate the possibility of a scaling-down philosophy. Medical computer tomography with a resolution of about half a millimetre on samples as big as core material can be used to quantify largest variations of coal macerals. Microfocus computer tomography can handle specimens up to 3 or 4 cm. The smaller the sample the better the achieved resolution, with an optimum of 10 μm in three dimensions. This allows visualising and quantifying smaller variations in composition.

7. Conclusion

Microfocus computer tomography is a very powerful technique for 3D coal characterisation. Beam hardening, the major artefact inherent to the technique of computer tomography, can be diminished by means of hardware filters, especially for low-attenuating materials like coal. Once a good image quality is achieved, a correlation with 2D colour image analysis of the surface can be performed. This study illustrated a serious gain in resolution compared to former studies of Verhelst et al. (1996) and Simons et al. (1997). Such a resolution enhancement is the most important parameter in calculating exact attenuation coefficients and densities of the macerals. Apart from this resolution enhancement and artefact reduction, a dual-energy technique enables us to extract physical density data rather than attenuation coefficients. This proved to be a very efficient means of extracting quantitative information about macerals. The overestimation of the density of liptinite forced us to characterise the mineral matter in the sample. Back-scatter electron microscopy and microfocus computer tomography revealed a strong interrelation of liptinite and clay minerals, which explains the overestimation in density. Finally, the 2D correlation of μCT data with data of CIA and BSE is the basis for an extension towards 3D characterisation of coal. This leads to the possibility of the visualisation of the distribution of coal components in 3D. Moreover, a quantification of the amount of components is possible.

Acknowledgements

The purchase of the Skyscan microfocus computer tomography system was financially supported by the Flemish Institute for the Promotion of the Scientific-Technological Research in the Industry (IWT), Project INM/950330. This research was financially supported by a grant of the Flemish Institute for the Promotion of the Scientific-Technological Research in the Industry (IWT). The scanning electron microscopic study is supported by Grant no. 2.0038.91 of the "National Fund of Scientific Research of Belgium". The authors also would like to thank Frederik J. Simons for his critical reading of the manuscript and journal referees Octavian Duliu and J.G. Prado.

References

Boespflug, X., Long, B.F.N., Occhietti, S., 1995. Cat-scan in marine stratigraphy: a quantitative approach. Mar. Geol. 122, 281–301.

Brooks, R.A., Di Chiro, G., 1976. Principles of computer assisted tomography (CAT) in radiographic and radioisotopic imaging. Phys. Med. Biol. 21, 689–732.

Coenen, J.C.G., Maas, J.G., 1994. Material classification by dual-energy computerized X-ray tomography. International Symposium on Computerized Tomography for Industrial Applications. Deutsche Gesellschaft für Zerstörungsfreie Prüfung e.v., Berlin, Germany, pp. 120–127.

Curry, T.S., Dowdey, J.E., Murry, R.C., 1990. Christensen's Physics of Diagnostic Radiology. Lea and Febiger, London.

David, P., Fermont, W.J.J., 1993. Application of color image analysis in coal petrology. Org. Geochem. 20, (6), 747–758.

Duliu, O.G., 1999. Computer axial tomography in geosciences: an overview. Earth Sci. Rev. 48, 265–281.

Fabre, D., Mazerolle, F., Raynaud, S., 1989. Caractérisation tomodensitométrique de la porosité et de la fissuration de roches sédimentaires. In: Maury, V., Fourmaintraux, D. (Eds.), Rock at Great Depth. Balkema, Rotterdam, pp. 297–304.

Finkelman, R.B., Gross, P.M.K., 1999. The types of data needed for assessing the environmental and human health impacts of coal. Int. J. Coal Geol., 40, 91–101.

Fuhrmann, G., 1993. Entwicklung eines Mikrotomographiesystems als Zusatz für Rasterelektronenmikroskope. Doctoral Thesis, Forschungszentrum Jülich, Jülich, Germany.

Harnett, D.L., Murphy, J.L., 1980. Introductory Statistical Analysis. Addison-Wesley Publishing, Reading, MA.

Herman, G.T., 1980. Image reconstruction from projections. The Fundamentals of Computerized Tomography. Academic Press, New York.

Jennings, R.J., 1988. A method for comparing beam-hardening filter materials for diagnostic radiology. Med. Phys. 15, 588–599.

Joseph, P.M., 1981. Artifacts in computed tomography. In: Newton, T.H., Potts, T.G. (Eds.), Radiology of the Skull and Brain: Technical Aspects of Computed Tomography, vol. 5, The CV Mosby Company, St. Louis, pp. 3956–3992.

Journel, A.G., Huijbregts, Dh.J., 1978. Mining Geostatistics. Academic Press, London.

Kak, A.C., Slaney, M., 1988. Principles of Computerized Tomographic Imaging. IEEE Press, New York.

Lamberson, M.N., Bustin, R.M., 1993. Coalbed methane characteristics of Gates Formation coals, Northeastern British Columbia: effect of maceral composition. Am. Assoc. Petrol. Geol. Bull. 77, 2062–2076.

Laxminarayana, C., Crosdale, P.J., 1999. Role of coal type and

rank on methane sorption characteristics of Bowen Basin, Australia coals. Int. J. Coal Geol. 40, 309–325.

Middleton, G.V., 2000. Data Analysis in Earth Sciences using Matlab. Prentice Hall, New Jersey.

Orsi, T.H., Edwards, C.M., Anderson, A.L., 1994. X-ray computed tomography: a nondestructive method for quantitative analysis of sediment cores. J. Sediment. Res. A, 64, 690–693.

Raynaud, S., Fabre, D., Mazerolle, F., Geraud, Y., Latière, H.J., 1989. Analysis of the internal structure of rocks and characterization of mechanical deformation by a non-destructive method: X-ray tomodensitometry. Tectonophysics 159, 149–159.

Sasov, A.Y., 1987. Microtomography: I. Methods and equipment. II. Examples of applications. J. Microsc. 147, 169–192.

Simons, F.J., Verhelst, F., Swennen, R., 1997. Quantitative characterization of coal by means of microfocal X-ray computed microtomography (CMT) and color image analysis (CIA). Int. J. Coal Geol. 34, 69–88.

Stach, E., Mackowsky, M.Th., Teichmüller, M., Taylor, G.H., Chandra, D., Teichmüller, R., 1975. Stach's Textbook of Coal Petrology. Gebrüder Borntraeger, Berlin.

Stonestrom, J.P., Alvarez, R.E., Macovski, A., 1981. A framework for spectral artifact corrections in X-ray CT. IEEE Trans. Biomed. Eng. 28, 128–141.

Swennen, R., Poot, B., Marchal, G., 1990. Computerized tomography as a tool in reservoir characterization. Zbl. Geol. Paläont. Teil I, 1105–1124.

Thomas, L., 1992. Handbook of Practical Coal Geology. Wiley, Chichester.

Van Geet, M., Swennen, R., Wevers, M., 2000. Quantitative analysis of reservoir rocks by microfocus X-ray computerized tomography. Sediment. Geol. 132, 25–36.

Verhelst, F., David, P., Fermont, W., Jegers, L., Vervoort, A., 1996. Correlation of 3D-computerized tomographic scans and 2D-colour image analysis of Westphalian coal by means of multivariate statistics. Int. J. Coal Geol. 29, 1–21.

Weisberg, S., 1980. Applied Linear Regression. Wiley, New York.

Wellington, S.L., Vinegar, H.J., 1987. X-ray computerized tomography. J. Petrol. Technol. 885–898.

Wenselaers, P., Dusar, M., Van Tongeren, P.C.H., 1996. Steenkoollaag methaanwinning in het Kempisch Kolenbekken: 'Het proefproject te Peer'. Ministerie van de Vlaamse Gemeenschap. ANRE, Brussel, Belgium.